ISSN 1064-2269, Journal of Communications Technology and Electronics, 2023, Vol. 68, No. 10, pp. 1219–1222. © Pleiades Publishing, Inc., 2023.
Russian Text © The Author(s), 2023, published in Radiotekhnika i Elektronika, 2023, Vol. 68, No. 10, pp. 1003–1007.

MICROWAVE ELECTRONICS

Design of Superconducting Integrated Matching Circuits[1]

F. V. Khan[a, b, *], A. A. Atepalikhin[a, b], L. V. Filippenko[a], and V. P. Koshelets[a]

[a] *Kotelnikov Institute of Radioengineering and Electronics, Russian Academy of Sciences, Moscow, 125009 Russia*
[b] *Moscow Institute of Physics and Technology (National Research University), Dolgoprudny, Moscow oblast, 141701 Russia*
**e-mail: khanfv@hitech.cplire.ru*

Received May 17, 2023; revised May 17, 2023; accepted May 25, 2023

Abstract—In this paper, we developed and investigated superconducting integrated circuits designed to match the impedances of a generator represented by a flux-flow oscillator based on a long Josephson junction and a detector based on a superconductor–insulator–superconductor tunnel junction in the subterahertz frequency range. The structures were modeled using the transfer matrix method. Designs were also calculated in the program of numerical three-dimensional modeling. A qualitative agreement was found between the results obtained by two methods. Three samples with different topologies were designed, covering the frequency range of 250–680 GHz at a level of –2 dB.

DOI: 10.1134/S1064226923100066

INTRODUCTION

To date, superconducting electronic devices have become widespread due to a set of unique characteristics that are unattainable for devices operating on other principles. Low noise temperature [1, 2], strong nonlinearity, operating frequencies in the terahertz (THz) region, as well as the possibility of integrating superconducting elements, all lead to the use of devices based on superconductor–insulator–superconductor (SIS) Josephson tunnel junctions as sources of THz radiation and receivers with high sensitivity. Such devices are used in various fields of science and technology, from the study of the composition of substances [3] to radio astronomy applications, such as the ALMA array of radio telescopes (https://almaobservatory.org) and the Millimetron project (https://millimeter.ru/).

Superconducting devices usually have the topology of planar integrated structures made on the same substrate together with the antenna and, in addition to tunneling Josephson junctions, also include microstrip lines with superconducting electrodes, through which the signal propagates and through which matching between circuit elements is carried out.

The best characteristics of generators and receiving elements are achieved, on the one hand, by improving the technology of sample fabrication [4]: in this way, modern methods of electon beam and optical lithography, ion etching, and magnetron sputtering make it possible to obtain high-quality junctions and achieve receiver noise temperatures of just a few times bigger the standard quantum limit in the THz frequency range ($T_{sq} = hf/k_B$, where f is the operating frequency). On the other hand, the operation of the devices essentially depends on the design of the structure. As shown in [5], multiple reflections from the SIS detector, resulting from the mismatch of the elements, lead to an increase in the noise temperature and narrowing of the intermediate frequency (IF) band.

In this paper, we calculate, study, and optimize niobium integral matching circuits in the frequency range of 250–700 GHz to ensure the best matching. The structures were calculated using a semi-analytical model based on the transfer matrix method and in the Ansys HFSS 3D numerical simulation program. The calculation results are compared with each other and with the experimental data for previously manufactured samples.

1. DESCRIPTION OF THE STUDY SAMPLES

An image of a superconducting microwave signal transmission line is shown in Fig. 1. A flux-flow oscillator (FFO) based on a long Josephson junction is used as a THz signal generator, the generation frequency is f, which is related to applied voltage V by known ratio: $hf = 2eV$ [6]. The detector in the circuit is made on the basis of a lumped SIS junction. Under the applied external alternating signal, the probability of tunneling of quasiparticles increases sharply and, as a result, the current increases at voltages below the gap voltage (so-called quasiparticle steps appear) [7]; this effect is used in experimental samples to estimate the incoming power. The current–voltage characteristic (IVC) of the SIS junction under the applied external

[1] The study was awarded a prize at the 19th Ivan Anisimkin Young Scientists Competition.

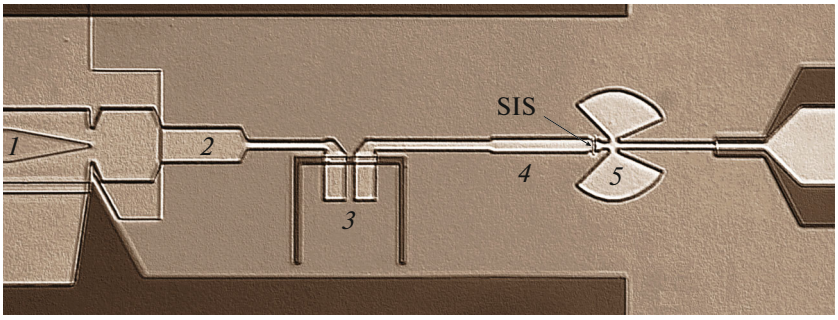

Fig. 1. A characteristic image of one of the superconducting integrated structures obtained with an optical microscope. The numbers indicate: (*1*) generator on the FFO, (*2*, *4*) step impedance transformers, (*3*) DC block in the form of a slot antenna, (*5*) a radial stub designed to adjust the capacitance of the SIS detector. The samples designed in this work differ from each other in the geometric dimensions of the elements inside each of the blocks *1*–*5*.

signal with a frequency of 400 GHz and the autonomous IVC are shown in Fig. 2. To ensure independent connection of the FFO and the SIS detector by direct current and the possibility of transmitting a microwave signal in a wide frequency band, there is a DC block in the line, made in the form of a slot antenna.

2. SIMULATION METHODS FOR SUPERCONDUCTOR INTEGRATED STRUCTURES

When designing superconducting integral matching structures, two models described in [8] were used. Both models are in good agreement with each other and with the experimental data for previously fabricated samples (Fig. 3).

2.1. Semi-Analytical Method

The first method is based on using transfer matrices (or ABCD matrices). In this method the fraction of the power coming from the generator to the detector is calculated [9, 10]. Each element of the structure is presented in the calculation as a quadripole with the corresponding matrix. When multiplying matrices in the order of the elements from the detector to the generator, the resulting matrix of the entire structure is obtained, from which, after transformations, coefficient S_{21} can be calculated.

Compared to a conventional microstrip line, additional effects arise in a superconducting line: partial penetration of the magnetic field into the electrodes of the transmission line and the resulting change in the phase velocity [11], as well as the appearance of strong

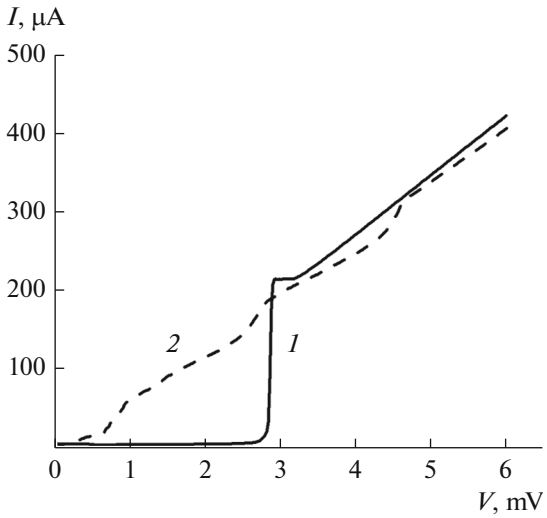

Fig. 2. Experimentally measured IVCs of the SIS junction used as a radiation detector: (*1*) autonomous IVC; (*2*) IVC under the influence of an external alternating signal with a frequency of 400 GHz.

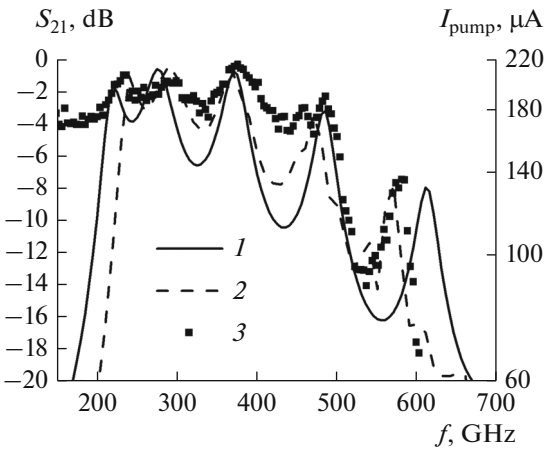

Fig. 3. Comparison of simulation results with experimental data for a sample made earlier: (*1*) is the frequency dependence of coefficient S_{21} obtained by semi-analytical calculation, (*2*) are the results of the numerical calculation; (*3*) experimentally measured values of pump current I_{pump} of the SIS detector depending on the FFO frequency.

attenuation of waves at frequencies close to the gap. These effects are taken into account using the separately calculated impedance per square surface of the upper and lower electrodes according to the formulas from the Mattis–Bardeen theory [12].

The developed program allows relatively fast calculation of the structure when changing the geometric size or another parameter of individual elements of the circuit (for example, the thickness of the insulation layer), which significantly speeds up the design and optimization process. In this regard, the development of new topologies of superconducting integrated circuits was carried out using this method.

2.2. Numerical Calculation in the 3D Modeling Program

In addition to the calculation using ABCD matrices, all the designed structures were simulated in the Ansys HFSS program; in HFSS, the Maxwell equations are solved in the entire modeled structure using the finite element method, and then coefficient S_{21} is found, corresponding to the ratio of the signal amplitude at the output port to the signal amplitude at the input, which can be interpreted (up to squaring) as the power coming from the generator to the detector. Modeling of superconducting elements and setting the corresponding boundary conditions were discussed in [13, 14].

Simulation of new samples made it possible, on the one hand, to verify the results of calculations obtained by the semi-analytical method, and, on the other hand, to show that both models lead to the same results for a wide class of structures.

3. TRANSMISSION LINE DESIGN

To match the FFO and the SIS detector through a DC block, stepped impedance transformers are used, made in the form of segments of microstrip lines with a length of $\lambda/4$, where λ is the wavelength of the radiation propagating along the line at the center of the matching band ($\lambda \sim 100$–300 μm).

In the simplest case of a single-step transformer, the best match between a generator with impedance Z_{gen} and load with impedance Z_l obtained if the characteristic impedance of the line is equal to $Z = (Z_{in}Z_l)^{1/2}$. To ensure matching between the SIS detector, the generator (absolute values of the order of a few fractions of an ohm) and the DC discontinuity (tens of ohms) in a wide frequency band, it is required to use transformers consisting of multiple sections; expressions for the characteristic impedance of each section can be found, for example, in [9]. At a constant thickness of the insulator layer and electrodes, the characteristic impedance depends on the width of the microstrip only. The width value is selected at the design stage.

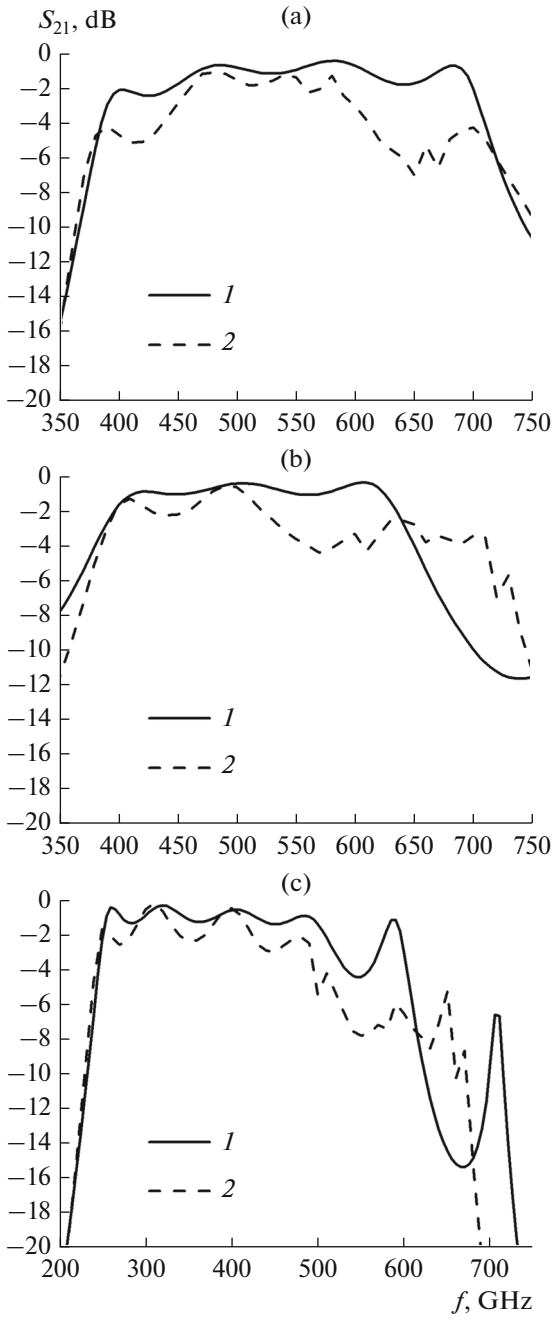

Fig. 4. S_{21} parameter dependences on frequency: (*1*) semi-analytical calculation; (*2*) numerical simulation; (a) design of a high-frequency line with a two-section transformer between the SIS detector and the DC block; (b) high-frequency line with a single-section transformer; (c) low-frequency line.

Previously, it was found that the bandwidth of matching the impedance of the SIS junction with the external structure depends on parameter χ, which shows the degree of shunting of the SIS junction [15]:

$$\chi = 2\pi f R_{HF} C S,$$

where f is the radiation frequency, R_{HF} is the high-frequency junction impedance (depending on the voltage

at the operating point), C is the junction capacitance per unit area (~0.08–0.09 pF/μm^2), and S is the transition area.

The characteristic value of parameter χ for an SIS junction with a normal resistance of 13 Ω and an area of 1 μm^2 at 400 GHz is about 2.8. The bandwidth of the impedance matching of the SIS junction with the structure is inversely proportional to parameter χ: $\Delta f \sim 1/\chi$. This encourages reducing its value, thereby expanding the operating range of frequency matching. One way to achieve small values of χ is to increase the tunneling current density of the Josephson junction by reducing barrier thickness d. Because dependence $R(d)$ is exponential, and dependence $C(d)$ is linear, then a significant decrease in resistance will lead to a slight increase in capacitance, and a decrease in product $R_{HF}C$.

4. DISCUSSION OF THE RESULTS

Figure 4 shows calculations of three designs of superconducting transmission lines covering the range of 250–680 GHz with a level no worse than –2 dB. A high-frequency line with the characteristic shown in Fig. 4a is made with a two-section transformer between the DC break and the SIS detector (see Fig. 1, position *4*). In another high-frequency line (Fig. 4b), a single-section transformer is used. S_{21} parameter dependency on the frequency shown in Fig. 4c corresponds to the low-frequency line. The results of semi-analytical calculation and numerical simulation are in qualitative agreement with each other.

CONCLUSIONS

The methods developed and tested on experimental samples for modeling superconducting transmission lines made it possible to optimize the topology of matching structures. Three samples were designed with a matching band of 360–680, 400–610, and 250–550 GHz at a level of –2 dB. A qualitative agreement is obtained between the results of numerical simulation and semi-analytical calculation.

ACKNOWLEDGMENTS

The authors are grateful for access to the equipment of the unique scientific unit "Cryointegral" (no. 352529), supported under the agreement of the Ministry of Science and Higher Education of the Russian Federation (RF-2296.61321X0041); the equipment was used in the manufacturing of samples and measurements.

FUNDING

The development of the manufacturing technology, the manufacture of samples, and the experiment were supported by the Russian Science Foundation, grant no. 23-79-00019, https://rscf.ru/project/23-79-00019/. Numerical calculations were supported by the state task at Kotelnikov IREE, RAS.

CONFLICT OF INTEREST

The authors of this work declare that they have no conflicts of interest.

REFERENCES

1. G. De Lange, D. Boersma, J. Dercksen, et al., Superconductor Sci. Technol. **23**, 045016 (2010). https://doi.org/10.1088/0953-2048/23/4/045016
2. B. Billade, A. Pavolotsky, and V. Belitsky, IEEE Trans. Terahertz Sci. Technol. **3,** 416 (2013). https://doi.org/10.1109/TTHZ.2013.2255734
3. N. V. Kinev, K. I. Rudakov, L. V. Filippenko, and V. P. Koshelets, Phys. Solid State **63**, 1414 (2021). https://doi.org/10.1134/S1063783421090171
4. M. Yu. Fominsky, L. V. Filippenko, A. M. Chekushkin, et al., Electronic **10** (23), 2944 (2021). https://doi.org/10.3390/electronics10232944
5. J. Y. Chenu, A. Navarrini, Y. Bortolotti et al., IEEE Trans. TST **6** (2), 223 (2016). https://doi.org/10.1109/TTHZ.2016.2525762
6. V. V. Shmidt, *Introduction to Physics of Superconductors* (MTsNMO, Moscow, 2000).
7. J. R. Tucker and M.J. Feldman, Rev. Mod. Phys. **57**, 1055 (1985). https://doi.org/10.1103/RevModPhys.57.1055
8. F. V. Khan, A. A. Atepalikhin, L. V. Filippenko, and B. P. Koshelets, J. Commun. Technol. Electron. **68** (9), 983 (2023).
9. V. F. Fusco, *Microwave Circuits: Analysis and Computer-aided Design* (Prentice-Hall, Englewood Cliffs, 1987; Radio i Svyaz', Moscow, 1990).
10. D. A. Frickey, IEEE Trans. Microwave Theory Tech. **42**, 205 (1994). https://doi.org/10.1109/22.275248
11. J. C. Swihart, J. Appl. Phys. **32**, 461 (1961). https://doi.org/10.1063/1.1736025
12. D. C. Mattis and J. Bardeen, Phys. Rev. **111**, 412 (1958). https://doi.org/10.1103/PhysRev.111.412
13. A. R. Kerr and S. K. Pan, Int. J. Infrared Millimeter Waves **11** (10), 1169 (1990). https://doi.org/10.1007/BF01014738
14. V. Belitsky, C. Risacher, M. Pantaleev, and V. Vassilev, Int. J. Infrared Millimeter Waves. **27** (1), 809 (2006). https://doi.org/10.1007/s10762-006-9116-5
15. K. K. Likharev, *Dynamics of Josephson Junctions and Circuits* (OPA, Amsterdam, 1986).